npj | antimicrobials & resistance

Article

https://doi.org/10.1038/s44259-025-00160-w

Computational framework for streamlining the success of sequential antibiotic therapy

Alejandro Anderson[1,5], Matthew W. Kinahan[2,5], Rodolfo Blanco-Rodriguez[1], Alejandro H. Gonzalez[3], Klas Udekwu[2] ✉ & Esteban A. Hernandez-Vargas[1,4] ✉

Antibiotic resistance represents a growing global health crisis, diminishing the effectiveness of existing treatments and accelerating the emergence of multidrug-resistant bacterial strains. In this study, we present a mathematical framework for systematically characterizing data sets of collateral sensitivity patterns in evolving drug-resistant bacterial populations. This formalization is implemented in an open-source computational platform providing an intuitive and accessible in silico tool for data-driven antibiotic selection. By leveraging this approach, we can rapidly identify a therapeutic regimen that minimizes the risk of resistance evolution. The utility of this framework is demonstrated by highlighting the failure of antibiotic therapy in chronic *Pseudomonas aeruginosa* infections. Our approach offers a scalable strategy for navigating bacterial evolutionary landscapes and delineates key conditions under which sequential antibiotic therapies are prone to failure.

The silent pandemic of antibiotic resistance is a pressing global health crisis, causing a high death toll[1–4]. While the discovery of new classes of antibiotics would be important, it is most likely that clinical resistance would evolve within years or decades[5–7].

Based on this scenario, a foundational interrogative would be if we can develop strategies for better treatment by using our current arsenal of antibiotics. Addressing this question would require the effective forecasting of bacterial evolution to personalized therapies known as "Evolutionary Therapies"[8]. Examples of this could be scheduling the order of antibiotics to take advantage of predictable patterns of bacterial evolution. This technology will enable stakeholders to empirically evaluate the risks associated with resistance evolution before drug administration[9]. To reach this quixotic but worthwhile endeavor, we need to develop computational models and analytical tools to predict how antibiotic resistance will likely evolve[10,11].

Evolutionary therapies have been developed by applying optimization methods to mathematical models of the evolving system[12–18]. Most antibiotic cycling strategies have been determined by linking dynamical models to fitness landscapes[12,14,15,19–22]. Other promising approaches are those based on reinforcement learning approaches, e.g.,[23], which are capable of learning effective drug cycling protocols. However, most machine learning algorithms require large data sets, thus basing the training on dynamically measured fitness landscapes. Another key obstacle from previous computational approaches is the assumption of a singular protein landscape - ignoring the inherent complexity of epistasis in both amino acid-, and gene-interactive networks. While this can facilitate analysis by Markov models[12] and other machine learning tools[23], the evolutionary constraint is limited to a number of mutations.

Collateral sensitivity, a phenomenon where a bacterium that has developed resistance to one antibiotic becomes more susceptible to another antibiotic, usually in a reversal of resistance phenotype. For example, a loss-of-function mutation in the efflux pump regulator *NfxB* in *Pseudomonas aeruginosa* leads to over-expression of the efflux pump MexCD-OprJ, granting ciprofloxacin resistance while simultaneously exhibiting collateral sensitivity to aminoglycosides[24]. These relationships are considered a potential key evolutionary loophole that can be exploited clinically, to combat antibiotic resistance with implications in the treatment of chronic infections, including long-term intensive care unit patients[25–29]. In such cases, disease-causing pathogens evade clearance by antibiotics and/or immune components. This can be due to multiple reasons, including but not limited to resistance mutations, bacterial persistence, and biofilm formation. Sequential antibiotic cycling has been used clinically to try to mitigate chronic infections, with mixed, albeit similar success rates as compared to antimicrobial combinations[30]. As chronicity would imply failure of clearance by two or more treatment regimens, collateral sensitivity consideration

[1]Department of Mathematics and Statistical Science, University of Idaho, Moscow, ID, USA. [2]Department of Biological Sciences, Bioinformatics and Computational Biology, University of Idaho, Moscow, ID, USA. [3]University of Littoral, Institute of Technological Development for the Chemical Industry and National Scientific and Technical Research Council, Santa Fe, Argentina. [4]Institute for Modeling Collaboration and Innovation, University of Idaho, Moscow, ID, USA. [5]These authors contributed equally: Alejandro Anderson, Matthew W. Kinahan. ✉e-mail: kudekwu@uidaho.edu; esteban@uidaho.edu

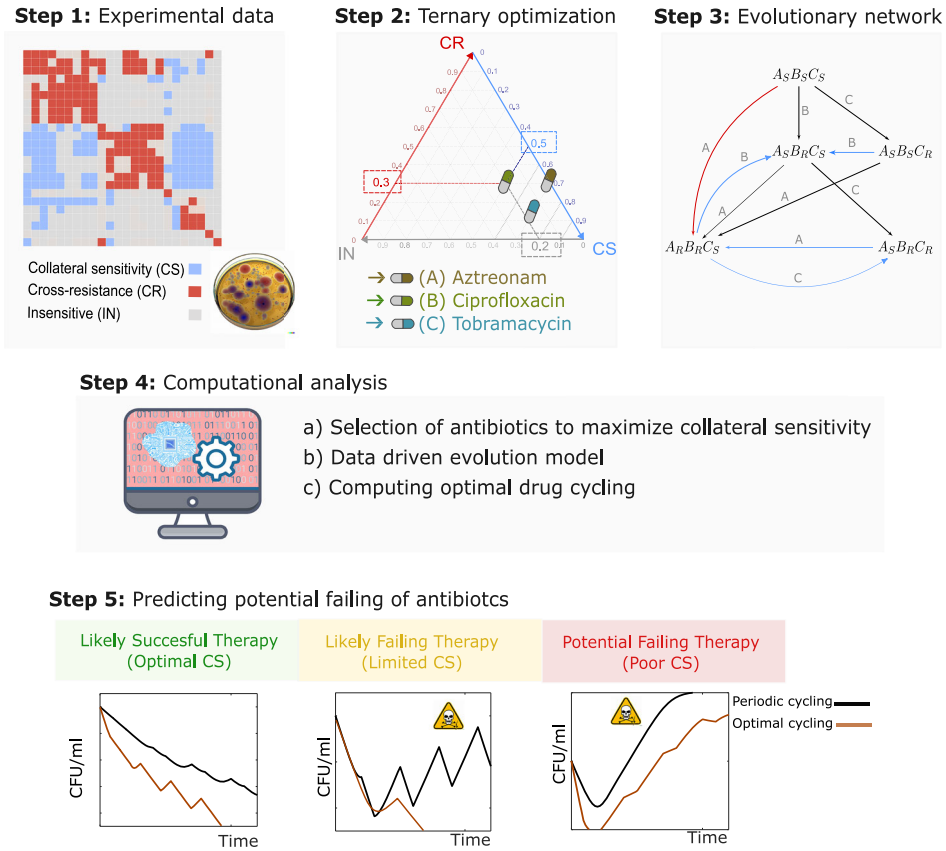

Fig. 1 | Interactive Collateral Sensitivity Platform. The computational platform requires the integration of MIC fold changes of the studied population as well as the selection of antibiotics to be evaluated (Step 1). Ternary plots are developed in Step 2 to identify the best selection of antibiotics to maximize collateral sensitivity. Based on the selection of antibiotics, a network model is constructed in Step 3. Ultimately, the network-based model is converted to a parametrizable dynamic model to optimize cycling therapies (Step 4). Predictions will highlight the potential failure of a cycling therapy (Step 5).

could prove to be invaluable for cases and infection types where standard treatment protocols have failed[31]. For this reason, we zoom in on chronic infections such as *Pseudomonas aeruginosa* lung infections, Gram negative pathogens involved in recurrent urinary tract infections, and *Staphylococcus aureus* cellulitis as a few examples. Cycling antibiotics based on collateral sensitivity presents an exceptional evolutionary therapy to tackle antibiotic resistance[28]. However, scheduling the order and time of antibiotics by trial and error is not feasible.

Recent mathematical models[18,32,33] show that collateral sensitivity-based dosing schedules could predict an effective antibiotic scheduling for suppression of within-host emergence of antibiotic resistance. The main drawback of previous modeling efforts is that they consider only hypothetical populations, *i.e.*, they are not data-driven.

In this paper, we conceive the mathematical formalization and its corresponding computational platform openly shared under FAIR principles[34], that performs data-driven prediction, to highlight the failure of a sequential combination of drugs, See Fig. 1. To utilize this platform, experiments where adaptive laboratory evolution to single drug resistance and subsequent changes in minimum inhibitory concentration, MIC, towards all other drugs under clinical consideration. Specifically, this framework was informed by chromosomal mutation data from ref. 35 and their results following the above-mentioned experimental procedure. To our knowledge, this is the first scalable framework to navigate collateral sensitivity to streamline antibiotic cycling. While our approach has limitations in predicting success, drugs that fail in this approach would fail in a realistic scenario.

Results

Our main contribution is the mathematical formalization of collateral sensitivity integrated into an intuitive and easy-to-use computational tool (Fig. 1) that serves to (i) avoid the selection of antibiotics that will trigger the emergence of a multi-resistant strain; (ii) derive data-driven dynamical models to navigate a subspace of the evolution landscape; and (iii) highlight antibiotic sequential failure.

It is worth emphasizing that our approach is based on a multivariable switched system of ordinary differential equations, which considers an instantaneous effect when a given drug is provided. While this approach is limited to providing the best sequence of drugs to eradicate a population, our predictions can highlight which antibiotics and therapeutic sequences to use in order to avoid triggering resistance. Thus, this platform would offer a conservative scenario. That is, if a drug combination fails within our platform, the same combination would fail if other clinical or microbiological criteria were included, such as pharmacodynamics and pharmacokinetics.

Our computational framework requires data as shown in Fig. 2, which shows drug susceptibility profiles of antibiotic-resistant bacteria relative to wild-type bacteria. The data set represents MIC fold changes of *P. aeruginosa* (PA01)[35] to 24 antibiotics (see Fig. 2); red for MIC fold increase (Cross-resistance, *CR*); blue for decrease (collateral sensitivity, *CS*); and gray for no change (insensitive, *IN*). The data set[35] was generated by evolving *P. aeruginosa* under drug exposure and characterization of the evolved resistance profile towards all other drugs in their study. Phenotypic susceptibility assays and whole genome sequencing were used to identify mutations associated with each resistance development. Subsequently, previous work[35] tested the susceptibility of resistant strains to alternative antibiotics by identifying instances of collateral sensitivity — where resistance to one drug increased susceptibility to another.

Mathematical formalism of collateral sensitivity

From collateral sensitivity observations[35], we can assume that the use of an antibiotic *A* will lead to the development of resistance to said antibiotic *A*. At the same time, the new population will be susceptible to an alternative antibiotic *B*, although initially resistant to antibiotic *B*. By this reasoning, any given collateral sensitivity, *CS*, can counteract a given resistance, *R*, to an

alternative drug. This relationship can be algebraically summarized as follows:

$$R : CS \rightarrow S \quad (1)$$

This is a nontrivial operation that requires careful consideration of the MIC fold differences needed to transition between what is defined as *R* (resistant) and *S* (susceptible) states. In our Methods section, we establish the mathematical details and assumptions to fulfill six evolutionary outcomes *R*: $CS \rightarrow S$; *R*: $CR \rightarrow R$; *R*: $IN \rightarrow R$; *S*: $CS \rightarrow S$; *S*: $CR \rightarrow R$; and *S*: $IN \rightarrow S$, relative to two states *R* and *S* for a variant, and three possible interactions *CS* (Collateral Sensitivity), *CR* (Cross-Resistance) and *IN* (Insensitive) for the antibiotics.

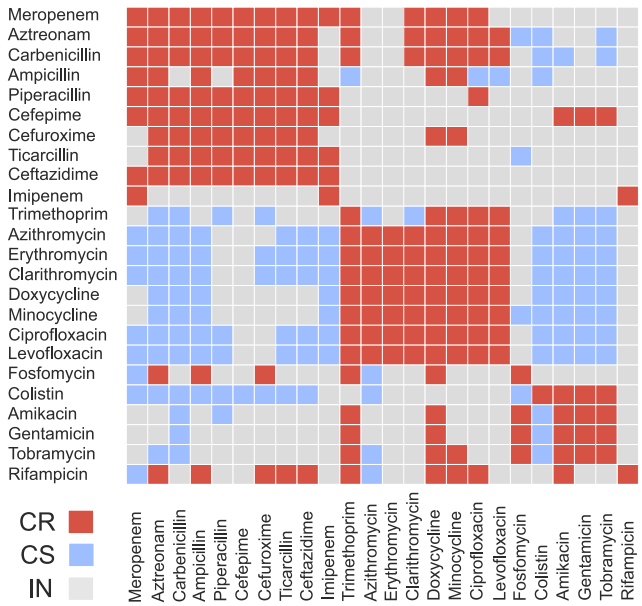

Fig. 2 | Collateral sensitivity plot for *P. aeruginosa* chronic infections. This plot is generated from experimental data from ref. 35. Rows delineate the profiles of a drug-evolved resistant strain. Each box represents the change in minimum inhibitory concentration (MIC) for PA01 on the column drug, with color indicating if evolved resistance to the row drug altered the MIC on the column drug compared to WT. Cross-resistance (CR) in red, collateral sensitivity (CS) in blue, and insensitive (IN) in gray.

As an illustrative example of the incorrect selection of antibiotics, Fig. 3 shows the effect of the interactions between antibiotics *Fosfomycin- FOS* (F), *Ceftazidime - CFZ* (C), *Amikacin-AMI* (A) and *Doxycycline-DOX* (D) on bacterial multiplication. Fig. 3A shows the collateral sensitivity plot of *P. aeruginosa* for these four antibiotics, extracted from the heatmap in Fig. 2. Observe in Fig. 3B how the wild-type strain $F_SC_SA_SD_S$ (susceptible to all drugs) is affected by antibiotic AMI (third row in the plot of Fig. 3A): because AMI shows *CR* towards DOX, the susceptibility of the wild-type to drug DOX, $F_SC_SA_SD_S$, develops resistance against DOX, $F_?C_?A_RD_R$, obtained by *S*: $CR \rightarrow R$ (the network is phenotype-based; an arrow *A* shows evolution under drug A exposure, and the resulting node displays resistance/sensitivity to other antibiotics). The "?" symbol reflects that our analysis has not yet focused on those drugs. Considering now the corresponding operation for drugs FOS and CFZ, a trend towards the strain $F_RC_SA_RD_R$ can be predicted, as depicted in Fig. 3B. The evolution of a population initially composed of the wild-type (10^9 number of bacteria) leads to the emergence of multidrug resistance, specifically the $F_RC_RA_RD_R$ variant, as observed after 12 days in Fig. 3C (red curve). This drives the exponential growth of the total population—which comprises the sum of all variants present in the evolutionary network—after day 21 (blue curve). In the computational simulations shown in Fig. 3C, which are based on Equation (11) described in Methods, each antibiotic exposure lasts 3 days per cycle for a total duration of 39 days.

Ternary diagrams for drug selection

Ternary diagrams provide a robust analytical framework for identifying optimal drug combinations within proximity of predefined therapeutic targets. The target position represents the desired proportional balance of collateral sensitivity, cross-resistance, and insensitive interactions among selected antibiotics.

The spatial coordinates within the ternary plots in Fig. 4, quantitatively reflect the interaction profile of each antibiotic through three orthogonal axes: collateral sensitivity (CS, depicted in blue), cross-resistance (CR, depicted in red), and insensitive interactions (IN, depicted in black). The proportional coordinates are calculated as the ratio of observed interaction type to the total number of evaluated antibiotics. For instance, in Fig. 4D, *colistin* (COL) occupies coordinates (*CS*, *CR*, *IN*) = (0.66, 0.33, 0), where the CS value of 0.66 represents the fraction of collateral sensitivity interactions relative to the total antibiotic panel (n = 3: *colistin*, *carbenicillin*, and *aztreonam*). This quantitative positioning enables systematic identification of antibiotic combinations that approximate desired therapeutic interaction profiles.

Our computational platform demonstrates optimal three-drug therapeutic combinations across six distinct targets within the ternary

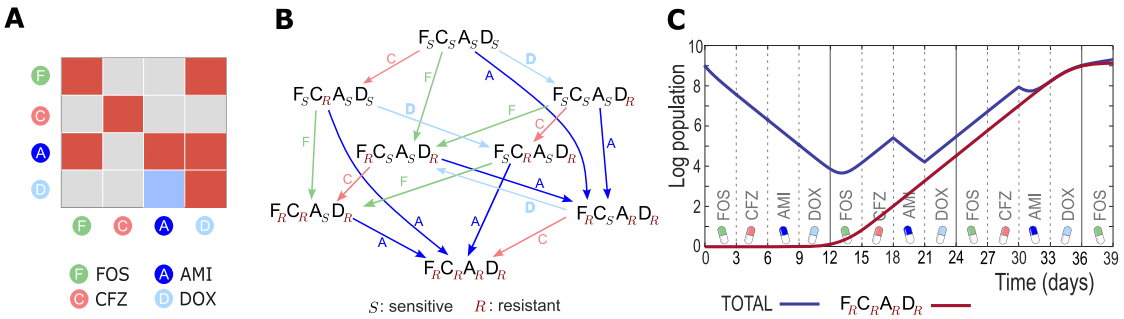

Fig. 3 | Example of inadequate antibiotics selection. The cycling protocol for antibiotics *Fosfomycin* (FOS), *Ceftazidime* (CFZ), *Amikacin* (AMI), and *Doxycycline* (DOX) consistently fails. **A** Collateral sensitivity plot of *P. aeruginosa* for antibiotics *F* = *FOS*, *C* = *CFZ*, *A* = *AMI*, and *D* = *DOX*, cross-resistance in red, collateral sensitivity in blue and insensitive in grey (data from[35]). **B** Evolutionary network associated with interactions between drugs *F*, *C*, *A* and *D*, for a population originally composed of the wild-type $F_SC_SA_SD_S$. The network uses collateral sensitivity data to show how drug stress promotes the selection of a specific bacterial variant. **C**. Dynamic evolution of the total population x_T (blue) and the multidrug resistant variant $F_RC_RA_RD_R$ (red), under a cycling protocol treatment. The cycle is defined by the ordered set *FOS* → *CFZ* → *AMI* → *DOX*, with a duration of 3 days per drug over a total exposure period of 39 days. The unavoidable escape of the population is attributed to multidrug resistant variant $F_RC_RA_RD_R$. The multidrug resistant variant $F_RC_RA_RD_R$ arises and grows exponentially after 12 days of sequential exposure to the antibiotics, leading to bacterial escape.

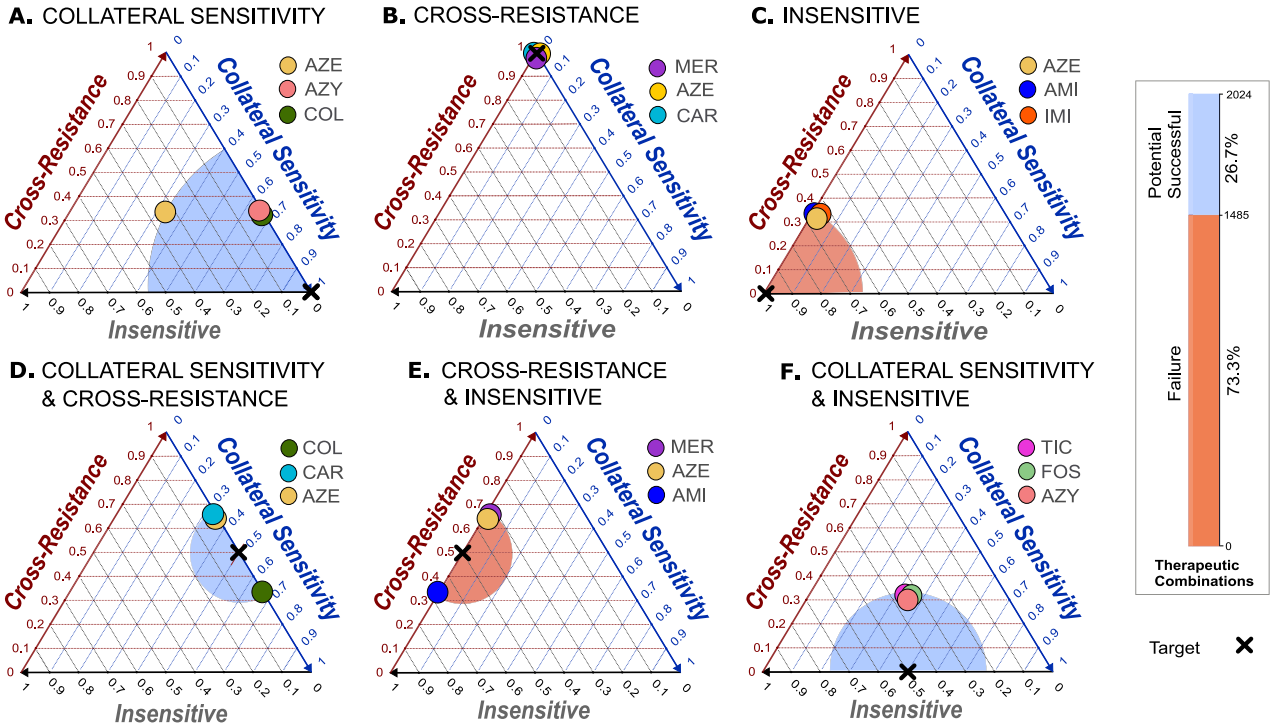

Fig. 4 | Ternary optimization for selection of three antibiotics. For three antibiotics, 2,024 different combinations are analyzed, corresponding to all (100%) possible combinations. **A** Antibiotics *Aztreonam* (AZE), *Azithromycin* (AZY), and *Colistin* (COL) are one solution exhibiting the highest level of collateral sensitivity, following a target given by 100% of collateral sensitivity. **B** *Meropenem* (MER), *Aztreonam* (AZE), and *Carbenicillin* (CAR) is among the solutions exhibiting the highest level of cross-resistance, following a target of 100% cross-resistance. **C**.*Aztreonam* (AZE), *Amikacin* (AMI), and *Imipenem* (IMI) are one solution exhibiting the highest level of insensitive, with a target given by 100% insensitive. **D** *Colistin* (COL), *Carbenicillin* (CAR), and *Aztreonam* (AZE) follow the target given by 50% collateral sensitivity and 50% cross-resistance. **E** *Meropenem* (MER), *Aztreonam* (AZE) and *Amikacin* (AMI) follow the target given by 50% cross-resistance and 50% insensitivity. Finally, **F** *Ticarcillin* (TIC), *Fosfomycin* (FOS), and *Azithromycin* (AZY) follow the target given by 50% collateral sensitivity and 50% insensitivity. The inset displays the total of 2,024 combinations for a three-drug therapy, of which 1485 combinations (73.3%) are associated with therapeutic failure, leaving only 539 cases to analyze their success. The shaded area represents the proximity of the solution to the target, red if the solution corresponds to therapy failure and blue otherwise.

parameter space (Fig. 4). The target configurations were strategically selected to represent diverse therapeutic scenarios, facilitating comprehensive exploration of the interaction data structure presented in Fig. 2. We systematically evaluated 2024 possible drug combinations, with 1485 combinations (73.3%) classified as treatment failures (Fig. 4, inset). Treatment failure classification was determined using established escape criteria (Supplementary Lemmas I and II), which define conditions under which multidrug-resistant variants emerge within the corresponding evolutionary network topology.

The solutions in each panel on Fig. 4 converge towards the target as closely as possible. Solution proximity to targets is quantified by shaded areas, where radius reflects the maximum drug-target distance. Red shading indicates treatment failure; blue indicates successful cycling protocols. Figure 4A showcases a therapeutic combination closely aligning with the highest level of collateral sensitivity, marked by the target 100%*CS*, 0%*CR*, and 0%*IN*. One solution includes *Aztreonam* (AZE), *Azithromycin* (AZY), and *Colistin* (COL). Notably, seven combinations out of the total 2, 024 exhibit identical interactions. The second panel, in Fig. 4B, identifies the set of antibiotics closer to the target 0%*CS*, 100%*CR*, and 0%*IN*. We show the solution *Meropenem* (MER), *Aztreonam* (AZE), and *Carbenicillin* (CAR), but there are 104 distinct combinations with the same interactions. The third panel, in Fig. 4C, shows that the set of antibiotics *Aztreonam* (AZE), *Amikacin* (AMI) and *Imipenem* (IMI), which demonstrates a higher level of insensitivity. The target here is 0%*CS*, 0%*CR*, and 100%*IN*, with 26 combinations with the same interactions. In panel Fig. 4D, the target 50%*CS*, 50%*CR*, and 0%*IN*, yields 17 solutions with the same interaction as *Colistin* (COL), *Carbenicillin* (CAR) and *Aztreonam* (AZE). The panel in Fig. 4E, with target 0%*CS*, 50%*CR*, and 50%*IN*, yields 133 solutions with the same interactions as *Meropenem* (MER), *Aztreonam* (AZE) and *Amikacin* (AMI). Finally, in Fig. 4F, the target 50%*CS*, 0%*CR*, and 50%*IN*, yield 3 solutions with the interactions as *Ticarcillin* (TIC), *Fosfomycin* (FOS), and *Azithromycin* (AZY).

Forecasting collateral effects in sequential therapy

Our platform integrates the evolutionary network into a dynamic system (Steps 3 - 4 Fig. 1) in which the switch to antibiotics shifts the balance of growth and death so that the population exposed to antibiotics shrinks or expands. The platform systematically predicts cycling protocol failure based on antibiotic interaction patterns, enabling high-throughput screening of combinatorial drug space and identification of viable therapeutic strategies.

Figure 5 demonstrates the temporal dynamics of bacterial growth under sequential antibiotic treatment in simulated populations initially composed of wild-type PA01. The model incorporates empirical susceptibility data for Pseudomonas aeruginosa from ref. 35, capturing population-level responses to antibiotic cycling protocols. Figure 5A depicts a cycling regimen involving antibiotics on panel Fig. 4A: AZE, AZY, and COL. The progressive decline of populations during the cycling treatment, is associated with the synergy among these antibiotics. A minor rebound is observed between days 18 and 21, which correlates with AZE's reduced collateral sensitivity (0.33) compared to AZY (0.66) and COL (0.66) (Fig. 4A). This temporal rebound suggests a substantial population fraction exhibits AZE resistance after 18 days. Figure 5B shows a cycling regimen with antibiotics on panel Fig. 4B:

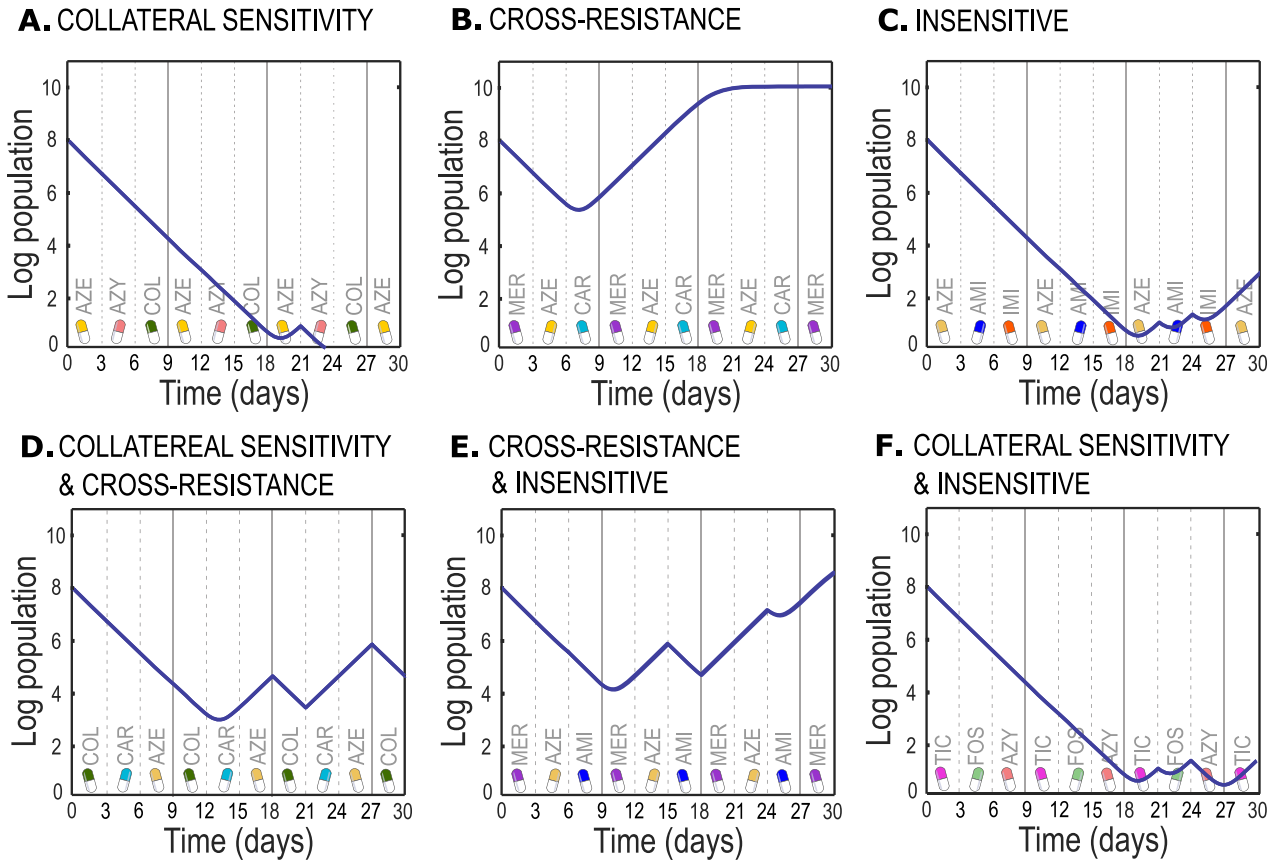

Fig. 5 | Qualitative long-term behavior of bacterial growth under cycling protocols. A Evolution of PA01 under a cycling of antibiotics *Aztreonam* (AZE), *Azithromycin* (AZY), and *Colistin* (COL), which exhibit the highest level of collateral sensitivity. **B** Prediction for cycling between *Meropenem* (MER), *Aztreonam* (AZE), and *Carbenicillin* (CAR), which exhibit the highest level of cross-resistance. **C** Cycling antibiotics *Aztreonam* (AZE), *Amikacin* (AMI), and *Imipenem* (IMI), which show a higher level of interaction. **D** Evolution of bacteria under cycling antibiotics *Colistin* (COL), *Carbenicillin* (CAR) and *Aztreonam* (AZE), which have 50% collateral sensitivity and 50% cross-resistance. **E** Evolution of PA01 under a cycling of antibiotics *Meropenem* (MER), *Aztreonam* (AZE), and *Amikacin* (AMI), which have 50% cross-resistance and 50% insensitivity. **F** shows bacterial grow for cycling *Ticarcillin* (TIC), *Fosfomycin* (FOS) and *Azithromycin* (AZY), which have 50% collateral sensitivity and 50% insensitivity.

MER, AZE, and CAR. These exhibit the highest degree of cross-resistance, leading to rapid evolution of resistance, and consequently, bacteria reach the carrying capacity after 21 days of exposure. This outcome aligns with predictions from the established escape criterion (Supplementary Lemma I). Figure 5C shows a cycling regimen with antibiotics on panel Fig. 4C: AZE, AMI, and IMI, which exhibit only insensitive interactions. There is a resistance delay; however, this set of antibiotics leads to treatment failure (population shows a rebound after day 18). This outcome aligns with predictions from the established escape criterion (Supplementary Lemma II). Figure 5D shows the cycling regimen with antibiotics on panel Fig. 4D: COL, CAR, and AZE, with cross-resistance and collateral sensitivity interactions, respectively. Bacteria evolve resistance toward CAR and AZE first, because COL displays higher collateral sensitivity. Figure 5-E depicts cycling regimen for antibiotics on panel Fig. 4E: MER, AZE, and AMI. This scenario is linked with failure based on the established escape criterion (Supplementary Lemma II). And Fig. 5F shows the cycling regimen for antibiotics on panel Fig. 4F: TIC, FOS, and AZY. These drugs exhibit 33% collateral sensitivity, 33% cross-resistance, and 33% insensitivity each. Bacteria evolve resistance toward TIC and FOS first; however, since all drugs have identical interactions, it is expected that bacterial escapes will occur after a longer period.

Computational simulations suggest drug interactions directly influence bacterial population dynamics, either promoting decay or facilitating proliferation. Notably, insensitive interactions represent a particularly problematic pattern in sequential antibiotic strategies: while initial bacterial load reduction may occur, accumulated resistance mechanisms ultimately enable population escape due to the emergence of multi-resistance.

The impact of order in sequential antibiotic therapy

The careful selection of antibiotics to formulate treatment regimens is paramount, as it significantly influences therapeutic outcomes. However, simple decisions on how to schedule medications can also be decisive. Figure 6 illustrates a computationally dynamic control analysis designed to highlight the impact of order in sequential therapies. In Fig. 6 we consider the impact of antibiotic cycle regimen of Carbenicillin (CAR), Erythromycin (ERI), Ampicillin (AMP), and Imipenem (IMI). Figure 6C and Fig. 6D show that the same drug combination when administered in a specific order can have enhanced efficacy compared to traditional sequential cycling. Simulations in Figs. 6A and B are initially comprised of the wild-type (10^9 number of bacteria). Further, each antibiotic exposure is constrained to last a minimum of 3 days per dosage. There is a pronounced difference in the susceptibility to a drug cycling designed to minimize population load compared to a traditional sequential drug cycling regimen even with the same antibiotics. The term *minimize* denotes a control strategy employed to determine the most effective order of antibiotic administration (refer to optimization details in Methods).

These findings highlight that order is a significant factor in preventing the emergence of resistance, and it can be decisive for the success or failure of sequential strategies.

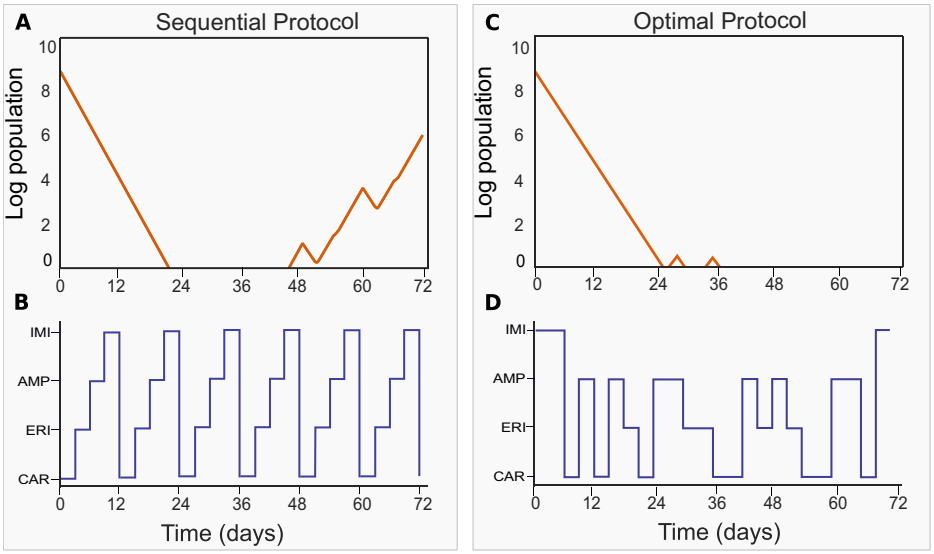

Fig. 6 | Total population dynamics for the sequential protocol (Panels A and B) and the optimal protocol (Panels C and D). A shows the total bacterial population under a sequential treatment with Carbenicillin (CAR), Erythromycin (ERI), Ampicillin (AMP), and Imipenem (IMI), as presented in (**B**). **D** illustrates how a non-trivial sequential order of the same drugs can contract and ultimately eradicate the total bacterial population, as shown in (**C**).

Discussion

The discovery that collateral sensitivity arises in bacterial populations following serial exposure to several antibiotics is a promising development in efforts to design drug-cycling protocols rationally. However, how best to apply the results of in vitro collateral sensitivity profiles obtained for bacterial pathogens is debatable, and how laboratory experiments can be used to inform treatment protocols deserves broader analysis. This can be attributed, at least in part, to the difficulty in translating such data.

In this study, we present an alternative approach to determining optimal drug combinations that highlights the failure of antibiotic combinations based on collateral sensitivity. Several studies have been carried out on the emergence of collateral sensitivity, and CS-interacting drugs were identified for *P.aeruginosa*[35], E. coli[28,29,36], and *E.faecalis*[37]. The predominant method of analysis has been a precursory application of network theory to identify CS interacting drugs and identify patterns of collateral sensitivity. While some common themes were obtained in the above-cited studies, e.g., CS of aminoglycoside-resistant mutants towards other antibiotics, the results are far from uniform.

To this end, we introduced a nuanced approach to classifying sequential drug combinations in a serially treated population of bacteria. In sequence, we (i) streamlined the analysis of collateral sensitivity data generated in vitro, simplifying experimental evolutionary outcomes defined by the evolutionary network and correlated MIC changes (see Fig. 2), (ii) formalized algebraically the defined phenotypic states (R or S) for $n \geq 2$ antibiotics, (iii) computed ternary diagrams that identified optimal combinations of interacting antibiotics (see Fig. 4), and (iv) simulated the population dynamics for each genotype component contributing to each sequential antibiotic protocol (Fig. 6).

The network approach commonly used in ref. 35 merely describes the interaction between drug-pairs, only casually referring to cycling protocols. While the magnitude of an infecting pathogen's MIC increase is informative, even small increments reduce the effective therapeutic window, which can result in treatment failure or from the microbial population's perspective, evolutionary escape. Here, we simplify the experimental 'training' data[35], focusing solely on the qualitative drug susceptibility classification of resistant *versus* sensitive.

In accordance with the non-trivial algebraic operation set out in Equation (1), we described the mathematical relationships between the various singly and multiply resistant components of a sequentially exposed population of an erstwhile sensitive (wt) bacteria. This is also applicable to cases where resistance is already present within the population[35]. Coupling these defined states into our birth and death-driven simulations, and following the emergent properties of the system for longer durations of time, we obtained a higher resolution of single and multiple drug-resistant populations in competition with the ancestral population. For some identified CS drug pairs in ref. 35, extended simulations using our modified framework led to treatment failure in silico. This observation is noteworthy especially where chronicity and episodic infections occur due to a resting population of quiescent bacteria with pathogenic properties.

Note that the implementation of collateral sensitivity in our study is conceptually similar[33], but it differs in several key aspects. Unlike previous modeling work[33], we do not incorporate pharmacokinetics or pharmacodynamics (PK/PD); consequently, our approach cannot evaluate drug effects on the population at the PK/PD level. However, it can rapidly identify drug combinations that are likely to fail in eradicating a population. Our mathematical models are grounded in experimental data, whereas previous models[33] considered only four genotypes and two drugs. In contrast, our framework scales to multiple genotypes and drugs, as demonstrated in our open-source platform. Moreover, our formulation is based on switched systems, which offer computational advantages for optimizing sequential therapies.

Sequential application of different drugs in such cases does not guarantee treatment success as subsequent evolution of an infecting pathogen to multi-resistance is often anticipated. We explore the utility of collateral sensitivity to create evolutionary networks for the assessment and prediction of optimal combinations of drugs that maximize pathogen clearance. To complement efforts to predict drug courses that can minimize the probability of resistance arising, we simplified the interaction between 'bug' and 'drugs' to a basic algebraic framework where resistance arising was deterministic.

Note that our platform utilizes the fold change MIC between a resistant population due to mutation in the chromosome or even in a plasmid-borne gene; the prerequisite experimental data would still hold, assuming there is no introduction of new genetic information[38].

For the first three steps of our platform presented in Fig. 1, our findings are not sensitive to the specific parameter values, since the framework relies only on the binary classification of a strain as sensitive or resistant. Thus, the results presented in Figs. 4 and 5 would remain unchanged under different parameter values. In contrast, parameter values do influence the temporal evolution of the system, as shown in Fig. 6, by affecting the time scales of population dynamics. Nevertheless, our focus in this step is not to predict precise bacterial dynamics, but rather to identify trajectories in which combinations of antibiotics are likely to fail in eradicating the population. Importantly, our framework is intentionally designed to provide a conservative estimate of failure scenarios rather than predictions of successful eradication. In future work, this framework could be extended to

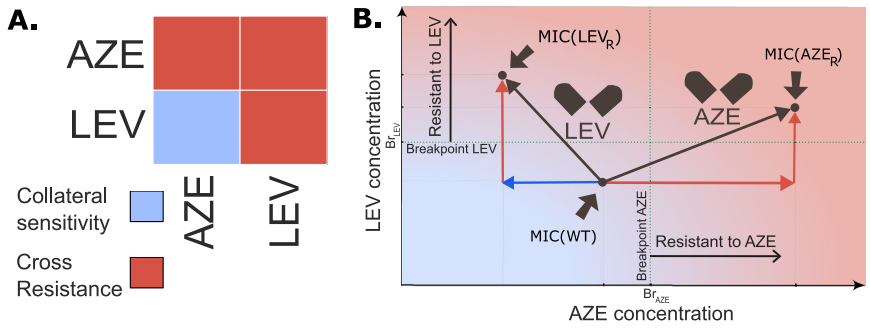

Fig. 7 | A Interactions between antibiotics Aztreonam (AZE) and Levofloxacin (LEV) for *P. aeruginosa*[35]: The first row delineates the profile of the AZE-evolved resistant strain AZE_R, which shows cross-resistance with respect to LEV; and the second row delineates the profile of the LEV-evolved resistant strain LEV_R, which shows collateral sensitivity with respect to AZE. B Quantifying collateral sensitivity: This two-dimensional concentration space for AZE and LEV, shows susceptibility and resistance regions colored by blue and red surfaces, respectively. The blue arrow represents collateral sensitivity, while the red arrows show cross-resistance. Reflecting on the MIC position, when stressed by antibiotic AZE, the wild-type (WT) strain evolves to variant AZE_R, becoming resistant to both drugs, as the MIC of AZE_R, $MIC(AZE_R)$, exceeds both breakpoints Br_{AZE} and Br_{LEV}. However, under LEV antibiotic stress, WT evolves to LEV_R, which remains sensitive to AZE but resistant to LEV, as the MIC of LEV_R, $MIC(LEV_R)$, only exceeds the breakpoint of antibiotic LEV, Br_{LEV}. This figure, reproduced from ref. 39, illustrates how different phenotypic states connect when a drug is active.

incorporate drug-specific PK/PD profiles and heterogeneous parameter values across antibiotics as in ref. 33. Such extensions would allow for a more refined, quantitative assessment of treatment outcomes while preserving the conceptual advantages of our approach.

In summary, our open-source computational platform, grounded in the principles of collateral sensitivity, offers a powerful tool for anticipating treatment failures in managing multidrug resistant bacterial infections. By predicting therapeutic failures and facilitating the selection of effective drug regimens, our platform provides a valuable step toward reducing antibiotic resistance in persistent infections.

Methods

Conceptualization of Susceptible (S) and Resistant (R) states for multiple antibiotics

Consider k antibiotics, $\{1,..., k\} = \Sigma$, and a given microorganism, x, the Minimum Inhibitory Concentration (MIC) parameter can be considered as k-dimensional as follows[39]:

$$MIC(x) = (MIC_1(x), \cdots, MIC_k(x)), \tag{2}$$

here, for a given antibiotic $\sigma \in \Sigma$, $MIC_\sigma(x)$ is the Minimum Inhibitory Concentration of drug σ for microorganism x.

In addition, Breakpoints represent the maximum concentration of all drugs allowed for use[40], and can be represented by:

$$Br_\Sigma = (Br_1, \cdots, Br_k), \tag{3}$$

here, the breakpoint Br_σ represents the maximum concentration of drug $\sigma \in \Sigma$ allowed for use.

It is important to note that our platform does not employ MIC fold-change thresholds directly. Instead, we use a simplified binary classification approach to highlight the direction of change (see Fig. 2): (i) Red (CR): MIC fold increase (cross-resistance), (ii) Blue (CS): MIC fold decrease (collateral sensitivity), (iii) Gray (IN): no significant change (insensitive). This framework captures qualitative trends in collateral responses without relying on absolute breakpoints, which can vary across bacterial species, antibiotics, and clinical guidelines.

Fig. 7B, reproduced from ref. 39, illustrates the MIC breakpoints for antibiotics, Levofloxacin (LEV) and Aztreonam (AZE). The MIC of the wild-type (Variant *WT*) indicates a profile of susceptibility to both drugs Fig. 7A. Under stress with antibiotic AZE, the *WT* evolves resistance towards the drug (population AZE_R), and the MIC of AZE_R increases concerning AZE and LEV; thus, the drug AZE shows cross-resistance to LEV. On the other hand, when exposed to antibiotic LEV, the *WT* evolves towards a resistant variant (LEV_R), and the MIC increases concerning LEV but decreases for AZE. In this case, drug LEV shows collateral sensitivity to AZE.

Following the methodology presented in ref. 39, susceptible and resistant phenotypic states can be defined for a set of antibiotics in Σ.

Definition 1. (Susceptible (S)/Resistant (R) phenotypic state[39]) Consider a microorganism x and k antibiotics, $\Sigma = \{1,..., k\}$. It is said that x is susceptible/resistant to drug $\sigma \in \Sigma$, if the σ^{th} element of the vector $MIC(x) - Br_\Sigma$, is negative/non-negative.

Accordingly, for a set of k antibiotics, a multidrug-resistant variant can be defined as follows:

Definition 2. (Multi-resistance) Consider a microorganism x and a set of k antibiotics, $\Sigma = \{1,\ldots, k\}$. The microorganism x is said to be *multi-resistant* to Σ if it is resistant to all antibiotics in Σ.

Collateral sensitivity patterns of antibiotics can be characterized as follows:

Definition 3. (Collateral effects[39]) Let $\Sigma = \{1,..., k\}$ denote a set of k antibiotics. Consider an antibiotic $\sigma \in \Sigma$ such that bacterial state x_i converges phenotypically to state x_j under selective pressure from antibiotic $\sigma \in \Sigma$, denoted $x_i \xrightarrow{\sigma} x_j$. Collateral effects can be represented by the drug-driven vector:

$$\vec{v} := MIC(x_j) - MIC(x_i). \tag{4}$$

If element i of $\vec{v}_\sigma$ is negative, then σ exhibits **collateral sensitivity** to antibiotic $i \in \Sigma$. If element i is positive, then σ exhibits **cross-resistance** to antibiotic $i \in \Sigma$. If element i of $\vec{v}_\sigma$ is zero, then σ exhibits **insensitivity** to antibiotic $i \in \Sigma$.

For a set of k antibiotics $\Sigma = \{1,..., k\}$, and two susceptibility profiles (S and R) for microorganism x with respect to each antibiotic, there are 2^k possible phenotypic states, (Supplementary Fig. 3). These 2^k states represent the distinct phenotypic variants, each differing from the others in its susceptibility profile with respect to at least one of the k antibiotics.

Evolutionary network for collateral sensitivity

Evolutionary network structures have previously been used to represent mutation pathways[39,41]. However, no formal methodology has yet been established to systematically compute a network that accounts for antibiotic cross-interactions. Here, a model network structure is constructed by integrating the antibiotic interactions landscape as a flow diagram[42], see Fig. 8. The nodes of the network are binary strings of length equal to the number of drugs for cycling protocol, let say $k \geq 2$. The σ-th element of the node can be

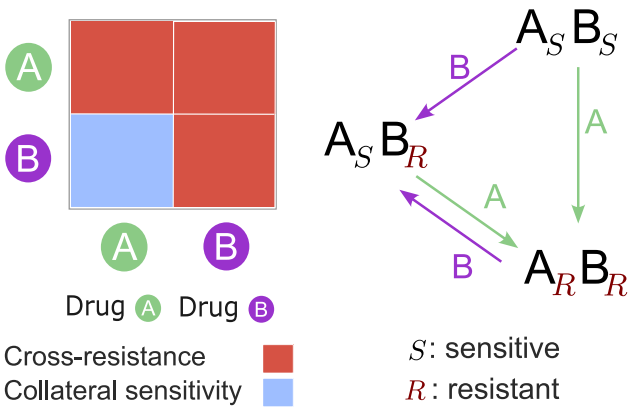

Fig. 8 | A hypothetical heatmap of drug *A* and drug *B* is shown on the left. Cross-resistance (CR) is indicated in red, while collateral sensitivity (CS) is shown in blue. Based on this heatmap, an evolutionary network can be constructed to represent the interactions between drugs *A* and *B*, starting from the wild-type A_SB_S (right). The subscript for each drug denotes whether the population is sensitive (S) or resistant (R). The direction of the arrows indicates how a given drug can drive the evolution of one population into another.

either sensitive (*S*) or resistant (*R*) to the σ-th drug of the list $\{1, 2, \cdots, k\}$. For instance, if $k = 6$ drugs, the node *RRRSSR* represents a microorganism resistant to drugs 1, 2, 3 and 6 but susceptible to drugs 4 and 5.

To construct the evolutionary network, we assume that exposure to an antibiotic induces resistance to that antibiotic, which is consistent with experimental data (see diagonal in Fig. 2). Additionally, interactions between antibiotics can be classified as collateral sensitivity (CS), cross-resistance (CR), or insensitivity (IN), each of which may influence transition rates between the nodes of the network. The connections between nodes can be modeled through the following assumption.

Assumption 1. For bacteria resistant (R) to antibiotic *B*, which are stressed by antibiotic *A*, the following holds:

i) If *A* has *CR* respect to *B*, the bacteria mutate to a new variant resistant to *B* (*R*: $CR \to R$).

ii) If *A* has *CS* respect to *B*, the bacteria mutate to a new variant sensitive to *B* (*R*: $CS \to S$).

iii) If *A* has *IN* respect to *B*, the bacteria mutate to a new variant resistant to *B* (*R*: $IN \to R$).

For bacteria sensitive (S) to antibiotic *B*, which are stressed by antibiotic *A*, the following holds:

iv) If *A* has *CR* respect to *B*, the bacteria mutate to a new variant resistant to *B* (*S*: $CR \to R$).

v) If *A* has *CS* respect to *B*, the bacteria mutate to a new variant sensitive to *B* (*S*: $CS \to S$).

vi) If *A* has *IN* respect to *B*, the bacteria mutate to a new variant sensitive to *B* (*S*: $IN \to S$).

We establish seed nodes as preexisting bacterial variants within the initial population (which could be just the wild-type). Upon sequential antibiotic exposure, these seeds generate drug-evolved resistant variants (emergent nodes), and the emergent nodes will be seeds for new nodes as well. The resulting network topology is sparse relative to the theoretical maximum of 2^k possible phenotypic states: node emergence depends on both the initial variant repertoire and antibiotic interaction profiles.

For example, Fig. 8 illustrates the evolutionary network based on the interactions between drug *A* and drug *B* and one seed, given by the wild-type A_SB_S (sensitive to *A* and *B*). Applying drug *A* to the seed A_SB_S directs the mutation towards node A_RB_R. Applying drug *B* to the seed A_SB_S directs the mutation towards node A_SB_R. Subsequently, applying drugs *A* and *B* to the emerging variants completes the evolutionary network, without the presence of variant A_RB_S.

The operators presented in Assumption 1:

$$R : CR \to R,\ S : CR \to R \tag{5}$$

$$R : CS \to S,\ S : CS \to S \tag{6}$$

$$R : IN \to R,\ S : IN \to S \tag{7}$$

provide a methodology to systematically characterize an evolutionary network for $k \geq 2$ antibiotics with 2^k nodes, as presented in Supplementary Fig. 3.

Ternary diagram for selection of antibiotics

A ternary diagram is constructed to illustrate the proportion between Collateral Sensitivity (CS), Cross-Resistance (CR), and Insensitivity (IN) across a set of *k* antibiotics, $\Sigma = \{1,..., k\}$. Each drug $\sigma \in \Sigma$ will have $a_\sigma \times 100\%$ of CS, $b_\sigma \times 100\%$ of CR and $c_\sigma \times 100\%$ of IN, with $a_\sigma + b_\sigma + c_\sigma = 1$. The position of antibiotic σ in the ternary diagram is given by $\mathbb{T}_\sigma = (a_\sigma, b_\sigma, c_\sigma)$. Figure 9 shows a heatmap for $k = 5$ hypothetical antibiotics and illustrates the construction of the ternary plot.

We utilize the ternary diagram to design an antibiotic selection system. Assume we aim to select *k* antibiotics $\Sigma = \{1,..., k\}$ from a list of $N = 24$ relevant antibiotics shown in Fig. 2, such that the chosen *k* antibiotics are as proximal as possible to a specific target point within the ternary diagram, Target = (T_{cs}, T_{cr}, T_{in}). The set $D(k, N)$ represents the collection of all possible combinations of *k* antibiotics from the total $N = 24$, such that $\Sigma \in D(k, N)$ implies $\sigma = \{1,..., k\}$ conformed by different antibiotics from the set of *N* available antibiotics. Consequently, $D(k, N)$ contains $\binom{N}{k}$ elements, where

$$|D(k, N)| = \binom{N}{k} = \frac{N!}{k!(N-k)!} \tag{8}$$

For any $\Sigma \in D(k, N)$, we can compute the ternary position for every $\sigma \in \Sigma$, represented by $\mathbb{T}_\sigma$. Then, every sequence of *k* drugs, given by Σ, has the following cost:

$$V(\Sigma,\ \text{Target}) = \sum_{\sigma=1}^{k} |\mathbb{T}_\sigma - \text{Target}|^2, \tag{9}$$

and we solve the optimization problem:

$$\Sigma^0 = \arg \min_{\Sigma \in D(k,N)} V(\Sigma,\ \text{Target}), \tag{10}$$

where Σ^0 is the sequence of *k* antibiotics closest to the Target = (T_{cs}, T_{cr}, T_{in}) point inside the ternary diagram.

Selecting *k* antibiotics entails evaluating $\binom{N}{k}$ possible combinations and identifying the combination that minimizes the cost function $V(\Sigma,$ Target). The cost function (9) penalizes the sum of relative Euclidean distances between antibiotic positions against a target point within the ternary diagram. By employing this method, we can evaluate a vast number of combinations and optimize the set of antibiotics to match the specified level of interactions we need closely.

Evolutionary dynamical model

The overall population dynamics are the outcome of two processes, the exponential decline of sensitive types (S) and the initially nearly exponential spread of resistant types (R). This process, called evolutionary rescue[43–45], delineates the foundational assumption upon which our dynamical analysis is built:

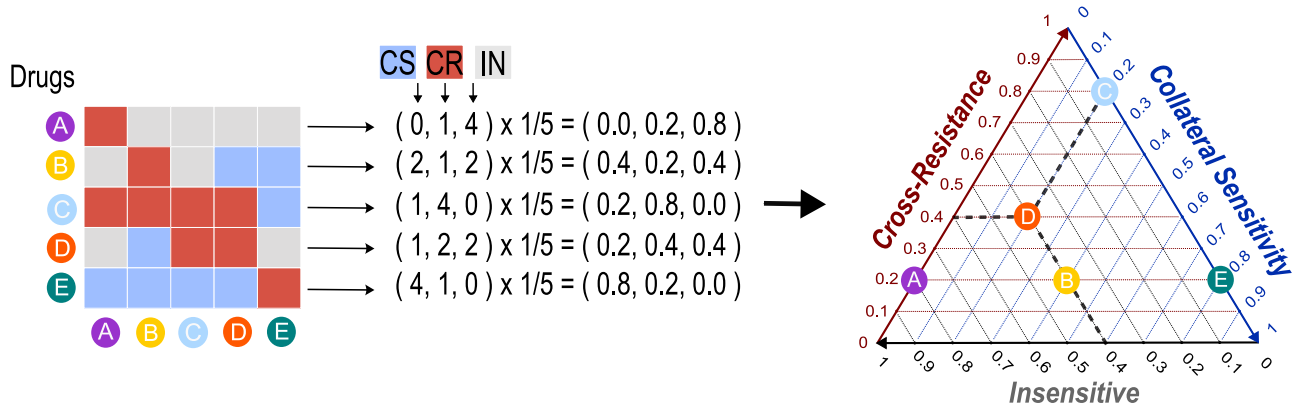

Fig. 9 | Ternary diagram construction. Profiles of drug-evolved resistant strains are shown in the left panel. In the middle panel, the number of blue (CS), red (CR), and grey (IN) blocks is counted and normalized by the total number of drugs. These normalized values define the coordinates of each drug in the ternary diagram (right panel).

Assumption 2. (Evolutionary rescue) In a sensitive bacterial population under antibiotic stress, the drug dose removes bacteria slowly enough for emerging resistant lineages to persist.

The assumption above has been widely modeled using an ODE system[32]. By considering two states, sensitive S and resistant R, with $\dot{R} = \alpha_R R\left(1 - \frac{S+R}{K}\right) - \delta_R R + \mu S$, and $\dot{S} = \alpha_S S\left(1 - \frac{S+R}{K}\right) - \delta_S S$; if there is an initial positive amount of state S, then state R emerges with a mutation rate μ.

Sequential antibiotic therapies can be formalized within the framework of switched dynamical systems, where the administration of different drugs corresponds to transitions between dynamical modes. In such systems, each mode is governed by its own equations of motion, while a switching signal specifies which mode is active at a given time[46]. When applied to bacterial populations, each mode naturally represents the dynamics under the selective pressure of a single antibiotic, and switching between drugs maps directly onto switching between modes[39,47,48].

The nodes of the evolutionary network, introduced in the previous section, correspond to n distinct bacterial variants, each defined by a unique susceptibility profile across the k antibiotics $\Sigma = \{1,..., k\}$ selected for cycling. These variants define the states of the switched system, denoted by x_i, $i = 1,\ldots, n$. Under pressure of antibiotic $\sigma \in \Sigma$, the rate at which the population x_i changes can be estimated by the addition of a growth, death and mutation terms.

Considering that α_i^σ and δ_i^σ represent the growth and death rates of state x_i under the action of antibiotic σ, respectively, we adopt the following qualitative assumption for the net growth rate:

Assumption 3. For a variant x_i exposed to antibiotic σ, we assume the net growth rate is negative, $\alpha_i^\sigma - \delta_i^\sigma < 0$, when x_i **susceptible** to σ; and we assume the net growth rate is non-negative, $\alpha_i^\sigma - \delta_i^\sigma \geq 0$, when x_i **resistant** to σ.

The collateral sensitivity evolutionary network described in the previous section can be represented by a family of k graphs, $G^\sigma(V, E)$, with one graph associated to each antibiotic $\sigma \in \Sigma$ (see example in Supplementary Fig. 3). The nodes $V = \{x_1,..., x_n\}$ correspond to the bacterial variants (states), while the edges E capture possible transitions between them. These connections are specified by the adjacency matrix entries m_{ij}^σ, of dimension $n \times n$, which describe the accessibility of variant x_j from variant x_i under the selective pressure of antibiotic σ (i.e., drug-driven transitions), where $m_{ij}^\sigma = 1$ indicates that a mutation from variant x_i to variant x_j is accessible under the selective pressure of antibiotic σ, and $m_{ij}^\sigma = 0$ otherwise.

The following equations estimate total bacterial size after a sequence of antibiotics given by the piecewise continuous function $\sigma(t)$: $[0, \infty) \to \{1, 2,..., k\}$:

$$\dot{x}_i(t) = \alpha_i^{\sigma(t)} x_i(t)\left(1 - \frac{x_T(t)}{K}\right) - \delta_i^{\sigma(t)} x_i(t) + \mu \sum_{j=1}^{n} m_{ij}^{\sigma(t)} x_j(t), \quad (11)$$

$$x_T(t) = \sum_{i=1}^{n} x_i(t) \quad (12)$$

where α_i^σ, δ_i^σ, and μ are growth, death, and mutation rates under pressure of drug σ, respectively. The state x_T denotes the total population, whose growth strictly depends on the resistant strains as they serve as the exclusive mechanism for the growth of x_T. Saturation of x_T is given by saturated population density K (carrying capacity).

Antibiotic treatment failure is frequently reported in randomized trials and observational studies as a measure of the inability to achieve the desired clinical response[49]. In the context of sequential therapy, failure occurs when bacterial pathogens survive successive interventions due to preexisting or newly acquired resistance mechanisms. This scenario can be interpreted as the presence or emergence of multidrug-resistant variants within the evolutionary network. Importantly, the dynamical model (11) enables the study of sequential antibiotic failure by examining the long-term behavior of the output x_T during the treatment regimen $\sigma(t)$[39]. Such failure is manifested by inability to control the total bacterial population size below levels associated with disease recurrence and reduced incidence of healthcare-associated infections[50].

Scheduling sequential antibiotics

From theory, we know that a switched system composed solely of unstable modes can stabilize the origin[46]. Biologically, this implies that although resistance persists (as stated in Assumption 2), it is theoretically possible to design a sequence of antibiotics that stabilizes the origin, thereby achieving treatment success. This insight is particularly important, as it suggests that cyclic treatments have the potential to effectively counteract the emergence of resistance.

To design a sequential therapy over the time interval $[0, T_f]$, k antibiotics must first be chosen. The switching times between one antibiotic and another are fixed and given by $0 = T_0 < T_1 < \cdots < T_{f-1} < T_f$, such that one antibiotic $\sigma_i \in \{1, 2,..., k\}$ is applied during the time interval $[T_i, T_{i+1})$. Then, the switching law is given by $\sigma(t) = \sigma_i$ for all $t \in [T_i, T_{i+1})$ for $i = 0, 1,..., f-1$. A switching law defined in this manner is said to be in the feasible set Σ_{T_f}. We want to find the switching law $\sigma(t) \in \Sigma_{T_f}$ that minimizes the following cost

function:

$$J(x(0);\sigma(\cdot)) = \int_0^{T_f} |x_T(t)|^2\, dt \tag{13}$$

for a given initial condition $x(0) = (x_1(0),..., x_n(0))$, and $x_T(t)$ given by Eq. (12). To do this, we solve the following problem:

$$\sigma^0(t) = \arg \min_{\sigma(t)\in\Sigma_{T_f}} \{J(x;\sigma(t)) : x = x(0)\} \tag{14}$$

Note that $\sigma^0(t)$ is the optimal solution that minimizes the total population growth x_T, considering only the order of the drugs. The optimization is performed by using the Differential Evolution (DE) algorithm[51], which is selected because of its simplicity and effectiveness.

Data availability

No new datasets were generated during the current study. We developed an open-source platform that provides an intuitive interface based on data on bacterial resistance profiles. Our tool enables rapid, data-driven decision-making to optimize therapeutic interventions. The complete source code is available in:https://github.com/systemsmedicine/Collateral-Sensitivity-Networks.

Received: 14 May 2025; Accepted: 1 October 2025;
Published online: 03 November 2025

References

1. Levy, S. B. The challenge of antibiotic resistance. *Sci. Am.* **278**, 46–53 (1998).
2. Mayers, D. L., Sobel, J. D., Ouellette, M., Kaye, K. S. & Marchaim, D.*Antimicrobial Drug Resistance: Clinical and Epidemiological Aspects*, vol. 2 (Springer, 2017).
3. Levy, S. B. & Marshall, B. Antibacterial resistance worldwide: causes, challenges and responses. *Nat. Med.* **10**, S122–S129 (2004).
4. Murray, C. J. et al. Global burden of bacterial antimicrobial resistance in 2019: a systematic analysis. *Lancet* **399**, 629–655 (2022).
5. Gold, H. S. & Moellering Jr, R. C. Antimicrobial-drug resistance. *N. Engl. J. Med.* **335**, 1445–1453 (1996).
6. Annunziato, G. Strategies to overcome antimicrobial resistance (amr) making use of non-essential target inhibitors: A review. *Int. J. Mol. Sci.* **20**, 5844 (2019).
7. Bollenbach, T. Antimicrobial interactions: mechanisms and implications for drug discovery and resistance evolution. *Curr. Opin. Microbiol.* **27**, 1–9 (2015).
8. Perry, G. H. Evolutionary medicine. *eLife* **10** (2021).
9. Rolff, J. et al. Forecasting antimicrobial resistance evolution. *Trends Microbiol.* (2024).
10. Stracy, M. et al. Minimizing treatment-induced emergence of antibiotic resistance in bacterial infections. *Science* **375**, 889–894 (2022).
11. Weinstein, R. A., Bonten, M. J., Austin, D. J. & Lipsitch, M. Understanding the spread of antibiotic resistant pathogens in hospitals: mathematical models as tools for control. *Clin. Infect. Dis.* **33**, 1739–1746 (2001).
12. Goulart, C. P. et al. Designing antibiotic cycling strategies by determining and understanding local adaptive landscapes. *PloS one* **8**, e56040 (2013).
13. Hernandez-Vargas, E. A., Colaneri, P. & Middleton, R. H. Optimal therapy scheduling for a simplified hiv infection model. *Automatica* **49**, 2874–2880 (2013).
14. Nichol, D. et al. Steering evolution with sequential therapy to prevent the emergence of bacterial antibiotic resistance. *PLOS Comput. Biol.* **11**, e1004493 (2015).
15. Mira, P. M. et al. Rational design of antibiotic treatment plans: a treatment strategy for managing evolution and reversing resistance. *PloS one* **10**, e0122283 (2015).
16. Yoon, N., Velde, R. V., Marusyk, A. & Scott, J. G. Optimal therapy scheduling based on a pair of collaterally sensitive drugs. *Bull. Math. Biol.* **80**, 1776–1809 (2018).
17. Tetteh, J. N., Matthäus, F. & Hernandez-Vargas, E. A. A survey of within-host and between-hosts modelling for antibiotic resistance. *Biosystems* **196**, 104182 (2020).
18. Nyhoegen, C. & Uecker, H. Sequential antibiotic therapy in the laboratory and in the patient. *J. Royal Soc. Interface* **20** (2023).
19. Toprak, E. et al. Evolutionary paths to antibiotic resistance under dynamically sustained drug stress. *Nat. Genet.* **44**, 101 (2012).
20. Visser, J. A. G. D. & Krug, J. Empirical fitness landscapes and the predictability of evolution. *Nat. Rev. Genet. 2014 15:7* **15**, 480–490 (2014).
21. Baym, M., Stone, L. K. & Kishony, R. Multidrug evolutionary strategies to reverse antibiotic resistance. *Science* **351**, aad3292 (2016).
22. Gjini, E. & Wood, K. B. Price equation captures the role of drug interactions and collateral effects in the evolution of multidrug resistance. *eLife* **10** (2021).
23. Weaver, D. T., King, E. S., Maltas, J. & Scott, J. G. Reinforcement learning informs optimal treatment strategies to limit antibiotic resistance. *Proc. Natl Acad. Sci. USA.***121** (2024).
24. Hernando-Amado, S. et al. Ciprofloxacin resistance rapidly declines in NFκB-defective clinical strains of Pseudomonas aeruginosa. *Nat. Commun.* **16**, 1–12 (2025).
25. Pluchino, K. M., Hall, M. D., Goldsborough, A. S., Callaghan, R. & Gottesman, M. M. Collateral sensitivity as a strategy against cancer multidrug resistance. *Drug Resist. Updates* **15**, 98–105 (2012).
26. Lázár, V. et al. Bacterial evolution of antibiotic hypersensitivity. *Mol. Syst. Biol.* **9**, 700 (2013).
27. Munck, C., Gumpert, H. K., Wallin, A. I. N., Wang, H. H. & Sommer, M. O. Prediction of resistance development against drug combinations by collateral responses to component drugs. *Sci. Transl. Med.* **6**, 262ra156–262ra156 (2014).
28. Imamovic, L. & Sommer, M. O. Use of collateral sensitivity networks to design drug cycling protocols that avoid resistance development. *Sci. Transl. Med.* **5**, 204ra132–204ra132 (2013).
29. Podnecky, N. L. et al. Conserved collateral antibiotic susceptibility networks in diverse clinical strains of Escherichia coli. *Nat. Commun.* **9**, 1–11 (2018).
30. van Duijn, P. J. et al. The effects of antibiotic cycling and mixing on antibiotic resistance in intensive care units: a cluster-randomised crossover trial. *Lancet Infect. Dis.* **18**, 401–409 (2018).
31. Casier, S. K., Lories, B. & Steenackers, H. P. Evolutionary drivers of divergent collateral sensitivity responses during antibiotic therapy. *Nat. Ecol. Evol.* 1–11 (2025).
32. Tetteh, J. N., Olaru, S., Crauel, H. & Hernandez-Vargas, E. A. Scheduling collateral sensitivity-based cycling therapies toward eradication of drug-resistant infections. *Int. J. Robust. Nonlinear Control* **33**, 4824–4842 (2023).
33. Aulin, L. B., Liakopoulos, A., van der Graaf, P. H., Rozen, D. E. & van Hasselt, J. C. Design principles of collateral sensitivity-based dosing strategies. *Nat. Commun.* **12**, 5691 (2021).
34. Wilkinson, M. D. et al. The fair guiding principles for scientific data management and stewardship. *Sci. Data* **3**, 1–9 (2016).
35. Imamovic, L. et al. Drug-driven phenotypic convergence supports rational treatment strategies of chronic infections. *Cell* **172**, 121–134 (2018).
36. Jahn, L. J., Munck, C., Ellabaan, M. M. & Sommer, M. O. Adaptive laboratory evolution of antibiotic resistance using different selection regimes lead to similar phenotypes and genotypes. *Front. Microbiol.* **8**, 1–14 (2017).

37. Maltas, J. & Wood, K. B. Pervasive and diverse collateral sensitivity profiles inform optimal strategies to limit antibiotic resistance. *PLOS Biol.* **17** (2019).
38. Herencias, C. et al. Collateral sensitivity associated with antibiotic resistance plasmids. *eLife* **10**, 1–13 (2021).
39. Anderson, A., Kinahan, M. W., Gonzalez, A. H., Udekwu, K. & Hernandez-Vargas, E. A. Invariant set theory for predicting potential failure of antibiotic cycling. *Infect. Dis. Model.* **10**, 897–908 (2025).
40. Kahlmeter, G. et al. European committee on antimicrobial susceptibility testing (eucast) technical notes on antimicrobial susceptibility testing (2006).
41. Komarova, N. L. & Wodarz, D. Drug resistance in cancer: principles of emergence and prevention. *Proc. Natl Acad. Sci.* **102**, 9714–9719 (2005).
42. Blanchini, F. & Giordano, G. Structural analysis in biology: A control-theoretic approach. *Automatica* **126**, 109376 (2021).
43. Bell, G. Evolutionary rescue. *Annu. Rev. Ecol., Evolu. Syst.* **48**, 605–627 (2017).
44. Ramsayer, J., Kaltz, O. & Hochberg, M. E. Evolutionary rescue in populations of pseudomonas fluorescens across an antibiotic gradient. *Evolut. Appl.* **6**, 608–616 (2013).
45. Drlica, K. The mutant selection window and antimicrobial resistance. *J. Antimicrob. Chemother.* **52**, 11–17 (2003).
46. Liberzon, D. *Switching in systems and control* (Springer Science & Business Media, 2003).
47. Hernandez-Vargas, E., Colaneri, P., Middleton, R. & Blanchini, F. Discrete-time control for switched positive systems with application to mitigating viral escape. *Int. J. Robust. Nonlinear Control* **21**, 1093–1111 (2011).
48. Anderson, A., Gonzalez, A. H., Ferramosca, A. & Hernandez-Vargas, E. A. Discrete-time MPC for switched systems with applications to biomedical problems. *Commun. Nonlinear Sci. Numer. Simul.* **95**, 105586 (2021).
49. Neill, R., Gillespie, D. & Ahmed, H. Variation in antibiotic treatment failure outcome definitions in randomised trials and observational studies of antibiotic prescribing strategies: a systematic review and narrative synthesis. *Antibiotics* **11**, 627 (2022).
50. Tong, S. Y., Chen, L. F. & Fowler Jr, V. G. Colonization, pathogenicity, host susceptibility, and therapeutics for Staphylococcus aureus: what is the clinical relevance? In *Seminars in immunopathology*, **34**, 185–200 (Springer, 2012).
51. Storn, R. & Price, K. Differential evolution-a simple and efficient heuristic for global optimization over continuous spaces. *J. Glob. Optim.* 341–359 (1997).

Acknowledgements

This material is based on work supported by the National Science Foundation under Grant No. DMS-2315862.

Author contributions

A.A. and M.K. shared the first author position. These authors contributed equally to this work. A.A., M.K., E.A.H.V., A.G., and R.B. developed the theory and performed the computations. E.A.H.V. and K.U. supervised the project. E.A.H.V. obtained the funding. All authors wrote and reviewed the manuscript.

Competing interests

The authors declare no competing interests.

Additional information

Supplementary information The online version contains supplementary material available at https://doi.org/10.1038/s44259-025-00160-w.

Correspondence and requests for materials should be addressed to Klas Udekwu or Esteban A. Hernandez-Vargas.